Product Operator Formalism

Wherever possible in this book, the simplest, non-mathematical treatment has been adopted. The majority of pulsed NMR experiments have been described in terms of extensions of the vector model* first introduced by Bloch. In a few applications, notably those involving multiple-quantum coherence*, this model breaks down, or at least has to be extended in an *ad hoc* manner. The general theory to describe the response to an arbitrary pulse sequence is the *density matrix* or *density operator* treatment (1,2). Unfortunately, this becomes very unwieldy for systems of several coupled spins, and very quickly gets out of touch with physical intuition which has been our principal guide in this book.

Fortunately, there is a more pictorial approach, championed by Sørensen *et al.* (3), which allows the new spin gymnastics to be treated formally without losing sight of the physical interpretation so important for our sanity. It is based on the decomposition of the density operator into a linear combination of products of spin angular momentum operators (4). It is applicable to weakly coupled spin systems. With this shorthand algebra, the fate of the various operators can be followed throughout a complex sequence of pulses and free precessions, throwing light on the details of the time evolution of the particular experiment. Lallemand (5) has suggested a tree-like pictorial representation to aid this kind of visualization.

For simplicity, we restrict ourselves here to the weakly coupled two-spin system IS, writing down the 16 product operators,

E/2	(where E is the unity operator)
I_X	X component of I-spin magnetization
I_Y	Y component of I-spin magnetization
I_Z	Z component of I-spin magnetization (populations)
S_X	X component of S-spin magnetization
S_Y	Y component of S-spin magnetization
S_Z	Z component of S-spin magnetization (populations)
$2I_XS_Z$	Antiphase I-spin magnetization
$2I_YS_Z$	Antiphase I-spin magnetization
$2I_ZS_X$	Antiphase S-spin magnetization
$2I_ZS_Y$	Antiphase S-spin magnetization
$2I_ZS_Z$	Longitudinal two-spin order
$2I_XS_X$	Two-spin coherence
$2I_YS_Y$	Two-spin coherence
$2I_XS_Y$	Two-spin coherence
$2I_YS_X$	Two-spin coherence.

The term $2I_XS_Z$ represents the X component of the I-spin magnetization split into two antiphase components corresponding to the two possible spin states of S. Such operators can be represented by the vector model but the last five product operators cannot be easily represented by vectors.

Longitudinal two-spin order $2I_ZS_Z$ is a specific disturbance of the populations of the four energy levels, having no net polarization. If the normal Boltzmann populations are represented as in Fig. 1(a), with population differences of 2Δ across each transition, then this *J-ordered state* has the populations indicated in Fig. 1(b). Both the I-spin doublet and the S-spin doublet have population disturbances such that a small flip angle read pulse would indicate an 'up–down' pattern of intensities. This is a common occurrence in certain polarization transfer* experiments.

Two-spin coherence $2I_XS_X$ is a concerted motion of the I and S spins that induces no signal in the NMR receiver coil, but can only be detected indirectly by two-dimensional spectroscopy*. It is a superposition of zero-quantum coherence (simultaneous I and S spin flips in opposite senses) and double-quantum coherence (flips in the same sense). Pure zero-quantum coherence corresponds to linear combinations of these product operators

$$2I_XS_X + 2I_YS_Y \text{ or } 2I_YS_X - 2I_XS_Y.$$

Pure double-quantum coherence corresponds to the alternative linear combinations

$$2I_XS_X - 2I_YS_Y \text{ or } 2I_XS_Y + 2I_YS_X.$$

We shall see below that one of the great strengths of the product operator formalism is its ability to account for experiments which involve multiple-quantum coherence.

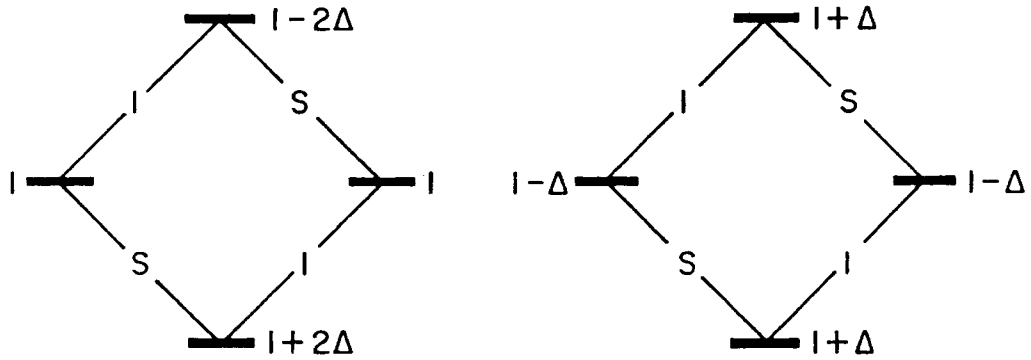

(a) Boltzmann equilibrium (b) Longitudinal two-spin order

Fig. 1. (a) Energy-level populations appropriate to a homonuclear IS spin system at Boltzmann equilibrium ($\Delta << 1$). (b) Populations corresponding to longitudinal two-spin order represented ! e product operator term $2I_ZS_Z$.

SIGN CONVENTIONS FOR ROTATIONS

For the vast majority of NMR experiments, the outcome is independent of the choice of the direction of precession of spins about magnetic fields. When using the vector model we adopted the widely used convention that (for a positive gyromagnetic ratio) a vector M rotates about a field in the rotating frame* as in Fig. 2. Thus for a radiofrequency field B_1 applied along the +X axis, a 90° pulse rotates $+M_Z$ to $+M_Y$

$$+M_Z \xrightarrow{90°(+X)} +M_Y. \qquad [1]$$

Similarly, we chose to take the sense of free precession to be clockwise looking down on the XY plane

$$+M_Y \rightarrow +M_X \rightarrow -M_Y \rightarrow -M_X \qquad [2]$$

for a Larmor frequency higher than the frequency of the rotating frame (ΔB positive). This convention simplifies diagrams of magnetization trajectories by concentrating on the front quadrant of the unit sphere.

When it comes to mathematical treatments using density operators or product operators, the sense of rotation is rather less of an academic point, and two opposite

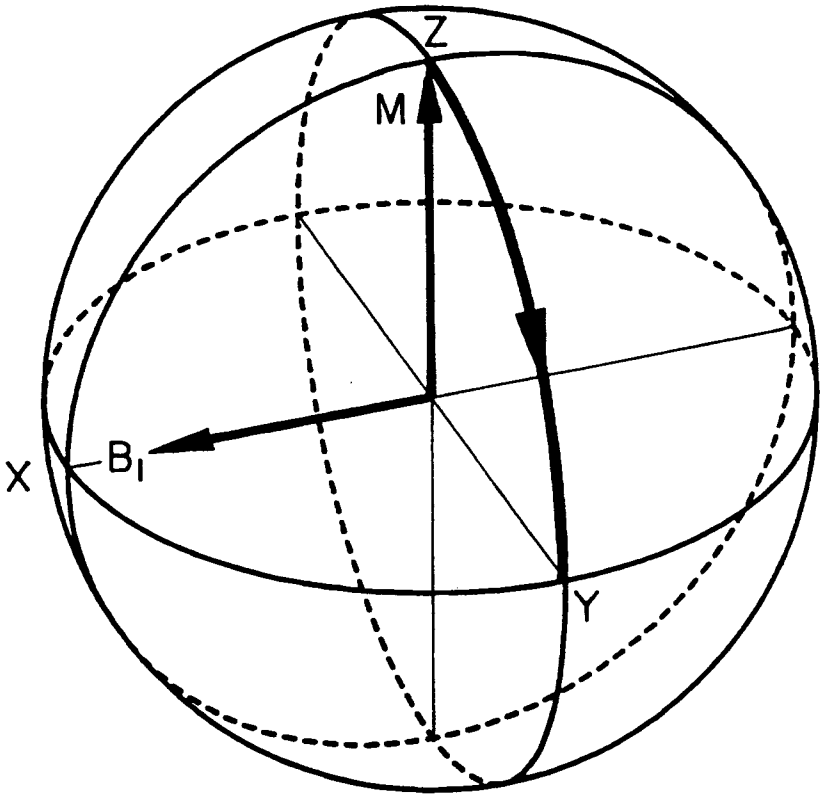

Fig. 2. Convention adopted for the sense of rotation of a magnetization vector M about a radiofrequency field B_1.

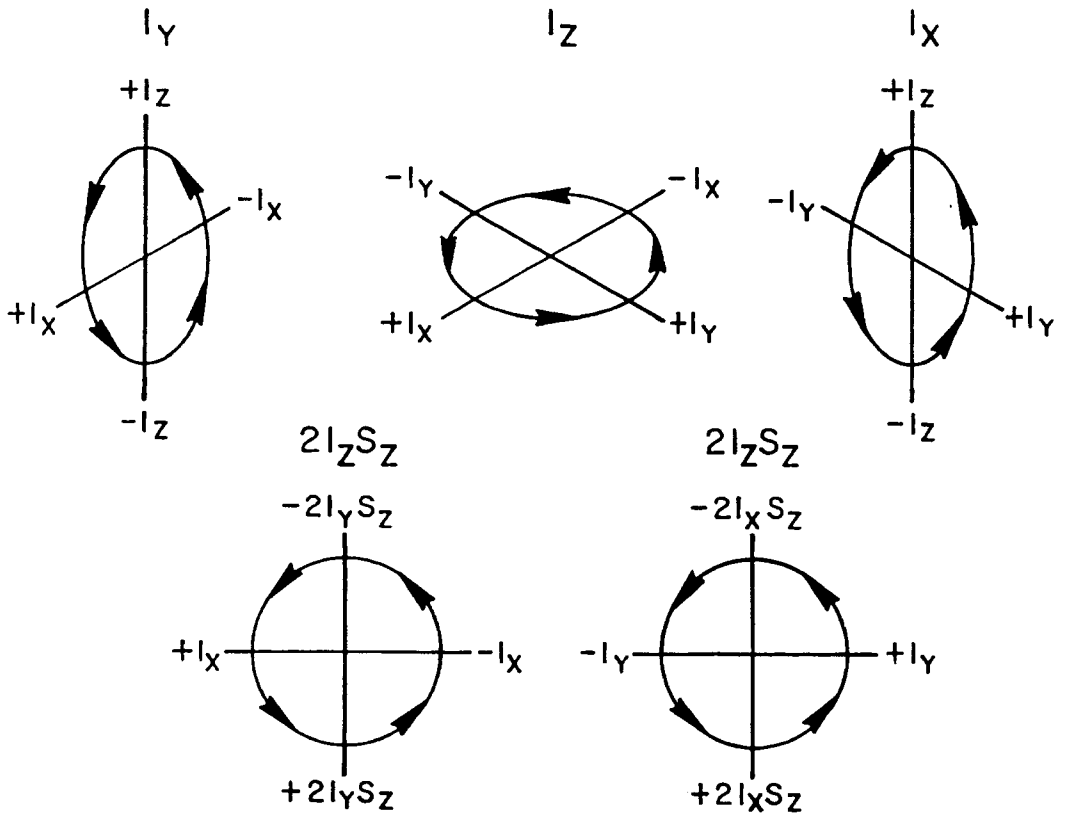

Fig. 3. Sign conventions for the evolution operators I_Y, I_Z, I_X and $2I_ZS_Z$ acting on the product operators I_X, I_Y, I_Z, $2I_XS_Z$ and $2I_YS_Z$. This schematic diagram is equivalent to Table 1.

schools of thought persist. Since the treatise of Sørensen *et al.* has become the standard article on the use of product operators in NMR pulse experiments, we adopt their sign convention, which is opposite to that of several other authors (2,5,6). In the product operator nomenclature, an operator (I_Z) is acted on by another operator I_X and the sign convention is *opposite* to that used above for magnetization vectors and fields (Fig. 3)

$$+I_Z \xrightarrow{+I_X} -I_Y. \qquad [3]$$

Similarly, a resonance offset effect causes a counter-clockwise rotation looking down on the XY plane

$$+I_Y \xrightarrow{+I_Z} -I_X \xrightarrow{+I_Z} -I_Y \xrightarrow{+I_Z} +I_X.$$

Finally, an operator $2I_ZS_Z$ has a specific sense of rotation

$$\begin{aligned} +I_X &\xrightarrow{+2I_ZS_Z} +2I_YS_Z \\ +I_Y &\xrightarrow{+2I_ZS_Z} -2I_XS_Z \end{aligned} \qquad [4]$$

These conventions are illustrated pictorially in Fig. 3 and embodied in Table 1.

Table 1. The effect of one of the evolution operators (top row) acting on one of the operators describing the state of the spin system (left-hand column).

	I_X	I_Y	I_Z	S_X	S_Y	S_Z	$2I_ZS_Z$
I_X	E/2	$-I_Z$	I_Y	E/2	E/2	E/2	$2I_YS_Z$
I_Y	I_Z	E/2	$-I_X$	E/2	E/2	E/2	$-2I_XS_Z$
I_Z	$-I_Y$	I_X	E/2	E/2	E/2	E/2	E/2
S_X	E/2	E/2	E/2	E/2	$-S_Z$	S_Y	$2I_ZS_Y$
S_Y	E/2	E/2	E/2	S_Z	E/2	$-S_X$	$-2I_ZS_X$
S_Z	E/2	E/2	E/2	$-S_Y$	S_X	E/2	E/2
$2I_ZS_Z$	$-2I_YS_Z$	$2I_XS_Z$	E/2	$-2I_ZS_Y$	$2I_ZS_X$	E/2	E/2
$2I_XS_Z$	E/2	$-2I_ZS_Z$	$2I_YS_Z$	$-2I_XS_Y$	$2I_XS_X$	E/2	I_Y
$2I_YS_Z$	$2I_ZS_Z$	E/2	$-2I_XS_Z$	$-2I_YS_Y$	$2I_YS_X$	E/2	$-I_X$
$2I_ZS_X$	$-2I_YS_X$	$2I_XS_X$	E/2	E/2	$-2I_ZS_Z$	$2I_ZS_Y$	S_Y
$2I_ZS_Y$	$-2I_YS_Y$	$2I_XS_Y$	E/2	$2I_ZS_Z$	E/2	$-2I_ZS_X$	$-S_X$
$2I_XS_X$	E/2	$-2I_ZS_X$	$2I_YS_X$	E/2	$-2I_XS_Z$	$2I_XS_Y$	E/2
$2I_XS_Y$	E/2	$-2I_ZS_Y$	$2I_YS_Y$	$2I_XS_Z$	E/2	$-2I_XS_X$	E/2
$2I_YS_X$	$2I_ZS_X$	E/2	$-2I_XS_X$	E/2	$-2I_YS_Z$	$2I_YS_Y$	E/2
$2I_YS_Y$	$2I_ZS_Y$	E/2	$-2I_XS_Y$	$2I_YS_Z$	E/2	$-2I_YS_X$	E/2

MANIPULATION OF PRODUCT OPERATORS

For the majority of pulsed NMR experiments in liquids, we are concerned with three main types of evolution – rotation by a radiofrequency pulse, rotation due to chemical shift, and rotation due to spin–spin coupling. Although the operation of a given pulse sequence clearly depends on the time ordering of the pulses and the intervening periods of free precession, during these latter periods we are at liberty to change the ordering of chemical shift and spin coupling evolutions, provided that the spin system is weakly coupled. The corresponding terms in the Hamiltonian are said to *commute*. We may speak of a *cascade* (7) of chemical shift or spin coupling terms where the time ordering is immaterial. Furthermore, a non-selective radiofrequency pulse acting on both the I and S spins may be broken down into a cascade of two pulses acting selectively on the I spins and the S spins, and the relative ordering does not matter.

RADIOFREQUENCY PULSES

During a radiofrequency pulse, the chemical shifts and spin–spin coupling constants can be imagined to be 'switched off' and the rotation is about an axis in the XY plane, normally the X axis. If necessary, we can consider rotation about a

tilted radiofrequency field B_{eff}. Consider, first of all, an excitation pulse $\beta(X)$ acting on the Z magnetization of the I spins, represented by I_Z. Thus

$$I_Z \xrightarrow{\beta I_X} I_Z \cos\beta - I_Y \sin\beta. \quad [5]$$

In the common example of a 90° pulse, this generates pure –Y magnetization; if it is a 180° pulse, there is a population inversion ($-I_Z$). Analogous expressions apply to pulses applied to the S spins, and for a non-selective pulse we would cascade the two rotations

$$+I_Z \xrightarrow{(\pi/2) I_X} -I_Y \quad [6]$$

$$+S_Z \xrightarrow{(\pi/2) S_X} -S_Y \quad [7]$$

A more complicated example occurs in the INEPT (8) experiment for polarization transfer in a heteronuclear IS system, commonly used to enhance the sensitivity of carbon-13 or nitrogen-15 spectra. In the key step of this sequence, I-spin magnetization vectors are prepared in an antiphase alignment along the ±X axes of the rotating frame and a $\pi/2$ pulse is applied to the I spins about the +Y axis. This rotation can be written as

$$2I_X S_Z \xrightarrow{(\pi/2) I_Y} -2I_Z S_Z \quad [8]$$

This creates longitudinal two-spin order, usually represented by I-spin vectors aligned along the ±Z axes. These population disturbances affect the S spins through the common energy levels, and these perturbations can be 'read' by a $\pi/2$ pulse applied to the S spins

$$-2I_Z S_Z \xrightarrow{(\pi/2) S_X} 2I_Z S_Y \quad [9]$$

We observe that the S-spin doublet has one line inverted and one line in the usual sense; in the case where the I spins are protons and the S spins are carbon-13, the 4:1 population advantage is transferred from protons to carbon-13, improving the sensitivity.

CHEMICAL SHIFTS

The evolution due to chemical shift effects may be represented by the operator equation

$$I_Y \xrightarrow{(2\pi\delta_I t) I_Z} I_Y \cos(2\pi\delta_I t) - I_X \sin(2\pi\delta_I t) \quad [10]$$

where δ_I is the shift of the I-spin resonance measured from the transmitter frequency. Note the sense of rotation is opposite to that used in the vector model.

Chemical shifts of the S spins are handled in analogous fashion. For heteronuclear systems a separate rotating reference frame is assumed for each spin, the chemical shifts being measured with respect to the appropriate transmitter frequencies in their respective frames.

SPIN–SPIN COUPLING

According to the vector model, spin–spin coupling causes a divergence of I-spin vectors at rates $\pm\frac{1}{2}J_{IS}$ with respect to a hypothetical vector precessing at the chemical shift frequency. In the product operator formalism coupling is represented by

$$I_Y \xrightarrow{(\pi J_{IS}\tau)\,2I_ZS_Z} I_Y\cos(\pi J_{IS}\tau) - 2I_XS_Z\sin(\pi J_{IS}\tau). \qquad [11]$$

If the interval τ is chosen such that $\tau = 1/(2J_{IS})$ then the cosine term is zero and we are left with

$$I_Y \xrightarrow{(\pi/2)\,2I_ZS_Z} -2I_XS_Z; \qquad [12]$$

that is to say, two I-spin magnetization vectors aligned in opposition along the $\pm X$ axes. We may then consider another period of free precession:

$$-2I_XS_Z \xrightarrow{(\pi J_{IS}\tau)\,2I_ZS_Z} -2I_XS_Z\cos(\pi J_{IS}\tau) - I_Y\sin(\pi J_{IS}\tau). \qquad [13]$$

If we make this second interval $\tau = 1/(2J_{IS})$ then we find that the two vectors are realigned along the –Y axis

$$-2I_XS_Z \xrightarrow{(\pi/2)\,2I_ZS_Z} -I_Y. \qquad [14]$$

With these simple rules the evolution of spin systems under the influence of a pulse sequence can be followed by evaluating the effect of the seven evolution operators I_X, I_Y, I_Z, S_X, S_Y, S_Z and $2I_ZS_Z$ on the operators describing the state of the spin system (15 in all). Table 1 shows the results. Then an 'evolution tree' can be constructed (5) where by convention each left-hand branch represents the cosine term of the evolution equations [5], [10], [11] or [13], while the right-hand side represents the sine term (evaluated from Table 1). When the two operators commute (E/2 in Table 1) then there is no change in that term. Note that the unaffected term is always associated with cosine; the affected term is associated with sine.

CORRELATION SPECTROSCOPY (COSY)

For the worked example we take the homonuclear correlation spectroscopy (COSY) for a system of two coupled spins I and S. This simple system illustrates the essential points; additional spins merely make the spectrum more complicated by increasing the number of resonances and by splitting the IS peaks through 'passive' couplings J_{IQ} and J_{SQ}, etc. A second important simplification is to drop S_Z from the initial density matrix, concentrating our attention on what happens to I_Z, since the problem is symmetrical with respect to the two spin systems.

The pulse sequence is deceptively simple:

$$90°(+X) - t_1 - 90°(+X) - \text{acquisition}\,(t_2). \qquad [15]$$

For the present purposes we may ignore the phase cycling* that is normally employed.

Chemical shift (I_Z) and spin coupling operators ($2I_ZS_Z$) may be applied in any order; in the acquisition period t_2 precession of the S spins is also considered, since by then there has been some transfer of coherence from the I spins. The evolution tree is set out in Fig. 4 showing the four stages of branching, leading to 13 terms in the final density operator. Of these, nine represent unobservable quantities – longitudinal magnetization (Z), multiple-quantum coherence (M) and antiphase magnetizations (A). It is the remaining four terms that are important; they can be grouped in pairs

$$D = \sin(2\pi\delta_I t_1)\cos(\pi J_{IS} t_1)\cos(\pi J_{IS} t_2)[I_X \cos(2\pi\delta_I t_2) + I_Y \sin(2\pi\delta_I t_2)] \quad [16]$$

$$C = \sin(2\pi\delta_I t_1)\sin(\pi J_{IS} t_1)\sin(\pi J_{IS} t_2)[S_X \cos(2\pi\delta_S t_2) + S_Y \sin(2\pi\delta_S t_2)]. \quad [17]$$

It is clear that D represents coherence that has precessed at frequencies close to the chemical shift δ_I in both t_1 and t_2. These are the *diagonal* peaks. The term in square brackets indicates that there is phase modulation in the t_2 interval. The significance

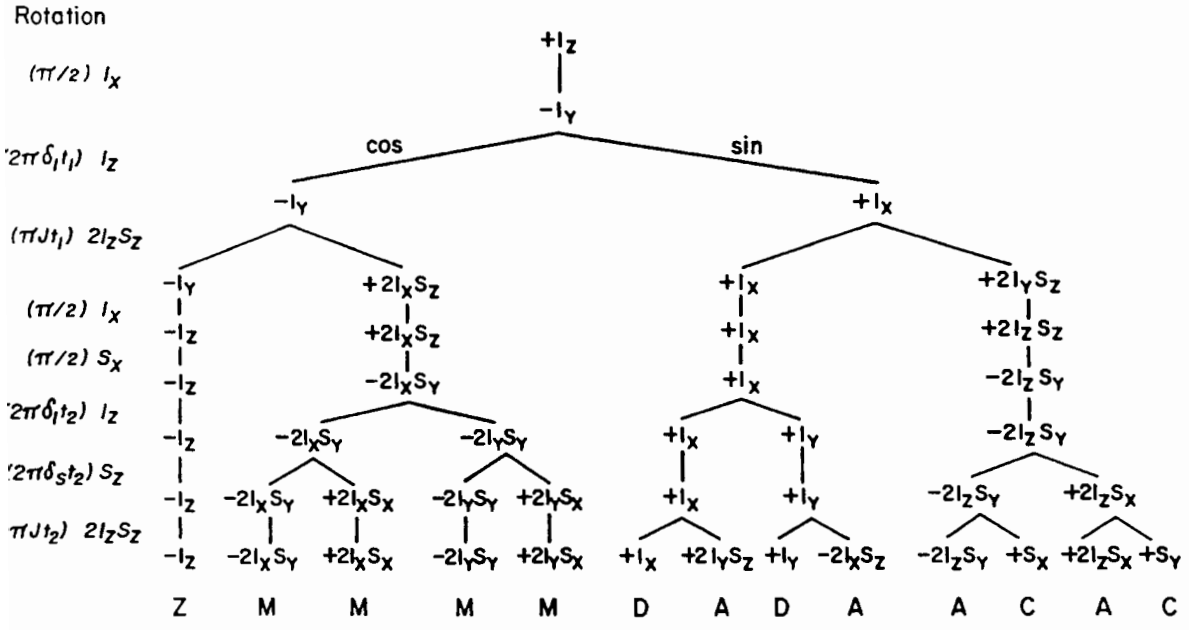

Fig. 4. Evolution of product operators appropriate to the homonuclear shift correlation experiment 'COSY'. For simplicity, the evolution of S_Z is omitted; it may be deduced from considerations of symmetry. Each left-hand branch implies multiplication by the cosine of the argument shown in the left-hand column, for example $-I_Y \cos(2\pi\delta_I t_1)$, while each right-hand branch implies multiplication by the corresponding sine term. The final 13 product operators are identified as Z magnetization (Z), multiple-quantum coherence (M), antiphase magnetization (A), diagonal peaks (D) or cross-peaks (C).

of the two J-modulation terms, $\cos(\pi J_{IS} t_1)$ and $\cos(\pi J_{IS} t_2)$, may not be immediately apparent. They may be converted by means of trigonometrical identities

$$\sin(2\pi\delta_I t_1)\cos(\pi J_{IS} t_1) = 0.5[\sin(2\pi\delta_I + \pi J_{IS})t_1 + \sin(2\pi\delta_I - \pi J_{IS})t_1]. \quad [18]$$

This represents a response in the F_1 dimension, centred at δ_I and split into a doublet (J_{IS}), both lines having the same phase. Similarly, the terms in t_2 may be combined to show that there is an in-phase doublet in the F_2 dimension. This is the familiar square pattern of lines straddling the principal diagonal.

By contrast, eqn [17] represents coherence that originated at frequencies near the chemical shift δ_I but which was detected at frequencies near δ_S, and thus describes one of the *cross-peaks*. (The other cross-peak would have been predicted by following the fate of S_Z, neglected in our calculation.) In this case the trigonometrical identity is

$$\sin(2\pi\delta_I t_1)\sin(\pi J_{IS} t_1) = 0.5[\cos(2\pi\delta_I - \pi J_{IS})t_1 - \cos(2\pi\delta_I + \pi J_{IS})t_1]. \quad [19]$$

This represents a response, centred at δ_I in the F_1 dimension, which is an antiphase doublet (J_{IS}). A similar identity shows that it is also an antiphase doublet in the F_2 dimension, centred at δ_S. The cross-peak is therefore a square pattern with the familiar intensity alternation. Normally we adjust the spectrometer phase so that the cross-peaks are in the absorption mode; then the diagonal peaks are in dispersion (sine modulation).

The presence of the terms $\sin(\pi J_{IS} t_1)\sin(\pi J_{IS} t_2)$ has another interesting consequence. It predicts that cross-peaks will have low relative intensities unless both t_1 and t_2 are permitted to evolve for times comparable with $(\pi J_{IS})^{-1}$, whereas the diagonal peaks will be relatively strong. This is important when searching for correlations based on very small coupling constants. Sometimes, a fixed delay is introduced into the evolution period in order to emphasize the effects of very small couplings (9).

Since this has been an illustrative exercise, all the evolutions have been worked out explicitly. Once familiarity with product operator algebra has been acquired, it is not normally necessary to carry through the calculation to the bitter end. For example, we could choose to stop the COSY calculation immediately after the second pulse ($t_2 = 0$), recognizing that the I_X term will give an in-phase doublet in the F_2 dimension and that the $-2I_Z S_Y$ term will evolve to give an antiphase doublet in F_2.

REFERENCES

1. A. Abragam, *The Principles of Nuclear Magnetism.* Oxford University Press, 1961.
2. C. P. Slichter, *The Principles of Magnetic Resonance.* Springer: Berlin, 1978.
3. O. W. Sørensen, G. W. Eich, M. H. Levitt, G. Bodenhausen and R. R. Ernst, *Prog. NMR Spectrosc.* **16**, 163 (1983).
4. U. Fano, *Rev. Mod. Phys.* **29**, 74 (1957).
5. J. Y. Lallemand, *École d'Été sur la Spectroscopie en Deux Dimensions,* Orléans, France, 1984.
6. U. Haeberlen, *High Resolution NMR in Solids, Selective Averaging.* Academic Press: New York, 1976.
7. G. Bodenhausen and R. Freeman, *J. Magn. Reson.* **36**, 221 (1979).
8. G. A. Morris and R. Freeman, *J. Am. Chem. Soc.* **101**, 760 (1979).
9. A. Bax and R. Freeman, *J. Magn. Reson.* **44**, 542 (1981).

Cross-references

Correlation spectroscopy
Multiple-quantum coherence
Phase cycling
Polarization transfer
Rotating frame
Two-dimensional spectroscopy
Vector model

Vector Model

Spin choreography is becoming more and more intricate. Many modern NMR experiments involve complex manipulations of nuclear magnetizations – enhancement, decoupling, correlation, refocusing, scaling, filtration, editing or purging. A simple scheme for visualizing these operations is therefore essential. The density operator theory is generally too cumbersome for the task, so many spectroscopists adopt the shorthand product operator formalism*, usually reduced to the bare minimum. Otherwise any intuitive insight is quickly lost if there are several coupled spins or if the manipulations become too complex. The vector model fills an important gap here, by permitting a ready visualization of possible spin manipulations, thus facilitating the task of devising new pulse sequences.

The vector picture is a natural extension of the classic treatment of magnetic resonance by Bloch (1,2) embodying the transient solutions of the Bloch equations. Although nuclear spins obey quantum laws, the ensemble average, taken over the very large number of spins in a typical sample, behaves just like a classical system, obeying the familiar laws of classical mechanics. We consider (initially) an isolated set of spin-$\frac{1}{2}$ nuclei in an intense field B_0 and represented by a single vector M, the resultant of all the individual nuclear magnetizations within the active volume of the sample. The motion is considered in a rotating frame* of reference, chosen such that the applied radiofrequency field $2B_1 \cos(\omega_0 t)$ can be represented as a static field B_1 aligned along the +X axis of this frame. The counter-rotating component of the radiofrequency field is ignored. In this frame the applied static magnetic field B_0 is reduced to a residual field

$$\Delta B = B_0 - \omega_0/\gamma \qquad [1]$$

so as to retain the Larmor precession condition.

At Boltzmann equilibrium, and in the absence of any recent radiofrequency excitation, the precession phases of individual spins are random and there is no resultant transverse magnetization ($M_{XY} = 0$). The longitudinal magnetization component M_0 reflects the slight excess of spins aligned along the field B_0 compared with those opposed to B_0. Most experiments start from this initial condition. In their simplest form, the Bloch equations tell us how the macroscopic magnetization vector reacts to the presence of the applied magnetic field and the temporary imposition of a radiofrequency field. At this stage we neglect relaxation effects.

$$dM_X/dt = \gamma(M_Y B_Z - M_Z B_Y) \quad [2]$$

$$dM_Y/dt = \gamma(M_Z B_X - M_X B_Z) \quad [3]$$

$$dM_Z/dt = \gamma(M_X B_Y - M_Y B_X). \quad [4]$$

This resolves the magnetization vector into its X, Y and Z components and considers their motion in the presence of magnetic fields B_X, B_Y or B_Z. If there is any magnetic field in the rotating frame, the nuclear magnetization vector M precesses around the field direction until that field is extinguished. For example, the familiar 90° excitation pulse is represented as a field B_X applied for such a duration that a vector M_0 along +Z is turned through 90° to the +Y axis of the rotating frame. Normally we are dealing with a hard pulse ($B_X = B_1 >> \Delta B$) so the residual field ΔB is neglected during the pulse. After the pulse the transverse nuclear magnetization vector precesses in the XY plane at a rate $\gamma\Delta B$ rad s^{-1}. In this case ΔB represents the chemical shift measured with respect to the transmitter frequency (the rotating frame frequency). A vector rotating in the XY plane intersects the receiver coil and induces a voltage which we call the free induction signal. The coil is, of course, in the laboratory frame, so we must add the frequency of the rotating frame, giving a result measured in hundreds of MHz, but the spectrometer reconverts this to an audiofrequency signal by subtracting the transmitter frequency (heterodyne action) so we are again dealing with the precession frequency in the rotating frame of reference.

In the more general case, the radiofrequency pulse may not satisfy the condition $B_1 >> \Delta B$, and we must consider an effective field

$$B_{eff} = (\Delta B^2 + B_1^2)^{1/2} \quad [5]$$

which is tilted in the XZ plane away from the +X axis through an angle θ given by

$$\tan\theta = \Delta B/B_1. \quad [6]$$

A radiofrequency pulse applied to an equilibrium magnetization vector then rotates the latter about the tilted effective field (see Radiofrequency pulses*).

Extensions of these simple manipulations can be represented by arcs on the surface of a unit sphere. In the presence of relaxation effects these magnetization trajectories must also include changes in length of the magnetization vector with time. This is achieved by treating relaxation *phenomenologically*, simply adding extra terms in the Bloch equations

$$dM_X/dt = \gamma(M_Y B_Z - M_Z B_Y) - M_X/T_2 \quad [7]$$

$$dM_Y/dt = \gamma(M_Z B_X - M_X B_Z) - M_Y/T_2 \quad [8]$$

$$dM_Z/dt = \gamma(M_X B_Y - M_Y B_X) + (M_0 - M_Z)/T_1. \quad [9]$$

This asks no questions about the nature of relaxation; T_1 is merely the time constant for the recovery of longitudinal magnetization, while T_2 is the time constant for the decay of transverse magnetization. Thus we see how thermal equilibrium is established when a sample is first placed in the magnetic field (eqn [9]), longitudinal relaxation carrying the instantaneous magnetization M_Z back to its equilibrium value M_0. It also describes how the transverse magnetization decays with time (eqns [7] and [8]), giving rise to a *free induction decay*.

We recognize, of course, that free induction signals usually decay much faster than predicted by the spin–spin relaxation rate. We now need another extension of the model, dividing up the sample into a mosaic of tiny volume elements called *isochromats* (2). These are large enough that they still contain a very large number of spins, but small enough that any gradients of the applied magnetic field can be neglected within an isochromat. The inhomogeneity of the applied field is thereby 'digitized', being represented by the slightly different Larmor frequencies of the different isochromats. Each isochromat is assigned a small vector m; their resultant is the macroscopic vector M. After a hard 90° pulse all the isochromatic vectors are in phase along the +Y axis, but they precess at different rates, fanning out in the XY plane and causing a decay of the detected NMR response. We normally represent this decay by a time constant T_2^*, the *instrumental* decay constant; this should not be confused with T_2. This picture clearly highlights the difference between the irreversible loss of magnetization through spin–spin relaxation and the dispersal of local isochromats, which can be reversed in a spin-echo* experiment.

EXTENSIONS OF THE BLOCH PICTURE

The Bloch equations were formulated at a time when high-resolution spectra with many different resonance lines were far in the future. Yet it can be very useful to extend these concepts to encompass several groups of chemically shifted nuclei, represented by independent vectors M_A, M_B,..., having the appropriate resonance offsets and relative intensities. Furthermore, the individual lines of a spin multiplet may also be assigned vectors, and they precess at frequencies which differ by the relevant spin–spin coupling constant. They can be labelled according to the spin states of the coupling partner, for example α and β for a doublet. We must therefore recognize that if this neighbour spin is inverted by a 180° pulse, the α and β labels are interchanged, and divergence becomes convergence (or vice versa).

This extension immediately suggests the concept of a selective (soft) radiofrequency pulse, one designed with a low-intensity B_1 (and correspondingly longer duration) so that it affects only one line (or close group of lines) without significantly perturbing the rest. We are then implicitly relying on the tilt of the effective field to discriminate between 'resonant' and 'non-resonant' situations: an effective field near the XY plane implies excitation, an effective field near the Z axis has little effect. We see that this can only be a relatively slow function of offset;

hence the need for shaped soft pulses with a more sharply defined transition between 'resonant' and 'non-resonant'. See Selective excitation*.

Such a picture has a reassuring parallel with the actual frequency-domain spectrum obtained by Fourier transformation. A vector M_A precessing at a frequency f_A in the XY plane during a free induction decay corresponds to a resonance at the frequency f_A Hz in the high-resolution spectrum and has an intensity proportional to M_A. If that particular vector decays with a time constant T_2 or T_2^* in the time domain, the corresponding resonance has a full linewidth of $1/(\pi T_2)$ or $1/(\pi T_2^*)$ Hz in the frequency domain. If we rotate the vector M_A through 180° (e.g. by a population inversion), the corresponding resonance line appears inverted. Note that we are implicitly assuming that each individual vector obeys the Bloch equations.

As new phenomena were discovered, the Bloch picture was adapted to include them. Slow chemical exchange carries spins from one site (A) to another site (B) with a different chemical shift. A population inversion of the spins at A therefore diminishes the length of the vector M_B as the inverted spins arrive at that site, but eventually M_B recovers its original length through spin–lattice relaxation. During exchange, spins departing from site A are replaced by B spins that have an essentially random phase. This can be reflected by introducing a new decay term into the relevant Bloch equation, for example

$$dM_Y/dt = \gamma(M_Z B_X - M_X B_Z) - M_Y/T_2 - M_Y/\tau \qquad [10]$$

where $1/\tau$ is the rate of chemical exchange. Analogous considerations apply to the nuclear Overhauser effect*; a rearrangement of spin populations brought about by cross-relaxation increases the length of a vector M_B when site A is saturated.

MAGNETIZATION TRAJECTORIES

Several important innovations in NMR methodology owe their inspiration to the intuitive application of the vector model. Tracing out the trajectory of a magnetization vector helps us understand certain types of pulse imperfection, for example the tilt effect of an off-resonance pulse. Levitt and Freeman (3) showed by drawing the appropriate magnetization trajectories that the error due to a tilt of the effective radiofrequency field could be largely compensated by combining three radiofrequency pulses into a composite pulse*

$$R = 90°(X)\ 180°(Y)\ 90°(X). \qquad [11]$$

This became the precursor of an entire family of self-compensating pulses that have enjoyed considerable success in many applications, for example broadband decoupling*.

In a similar manner, it is hard to imagine the discovery of the DANTE sequence (4) without being able to visualize the 'zig-zag' trajectories followed by an off-resonance spin, and the existence of multiple sideband resp[illegible]s follows neatly

from the vector picture. (See Selective excitation.) While it may now be common practice to rely on computer optimization techniques to design shaped soft radiofrequency pulses for (say) pure phase excitation (5), it will always be more satisfying to visualize the complex defocusing and refocusing effects by displaying families of magnetization vectors on the unit sphere.

At the heart of many modern spin manipulation schemes is some trick to separate interesting signal components from undesirable responses. Often this is achieved by phase cycling* or by the application of pulsed field gradients*. The former method discriminates between desirable and undesirable responses by distributing the corresponding vectors differently in phase space (usually along the four orthogonal directions in the XY plane), retrieving the interesting signals by cycling the receiver reference phase. The latter method spreads the various signal components in geometrical space through the application of a pulsed magnetic field gradient. Individual isochromatic vectors would then find themselves arranged in the form of a helix whose axis is the field gradient direction. The required signals are then collected by a suitable recall gradient that leaves the unwanted components still widely dispersed in space. The vector model is crucial to the understanding of both of these methods.

LIMITATIONS OF THE VECTOR MODEL

Not all experiments can be adequately treated by the vector model. One of the important cases where it breaks down (or at best involves too many *ad hoc* assumptions) is in the treatment of multiple-quantum coherence. The initial stage of this experiment is readily formulated as the preparation of two vectors α and β

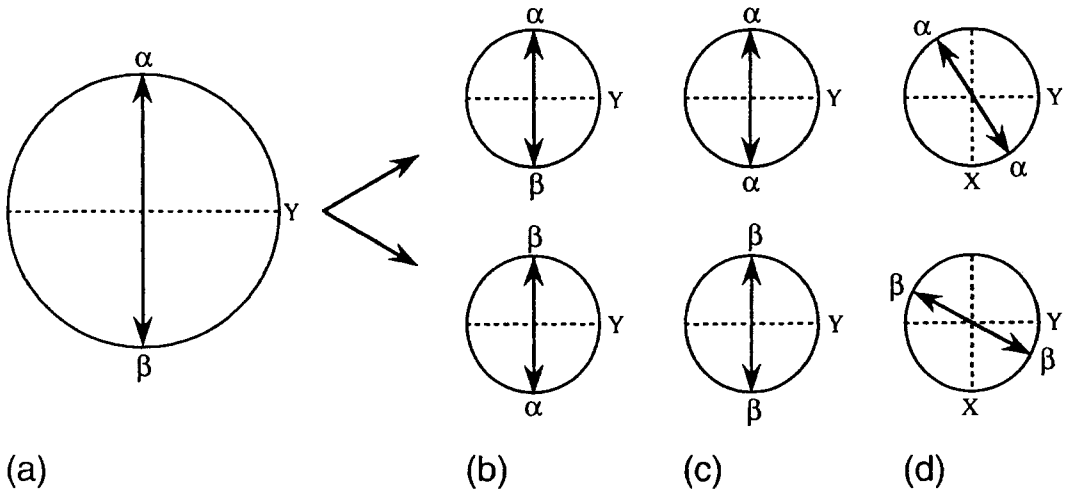

Fig. 1. Preparation and evolution of double-quantum coherence couched in terms of vectors. (a) The initial antiphase configuration of α and β vectors. (b) A 90° pulse applied to the coupling partner interchanges α and β labels for half of the spins. (c) Rearrangement of these vectors. (d) Evolution of double-quantum coherence by free precession of 'locked' vectors.

from a J-doublet in an arrangement where they are diametrically opposed along the ±X axes of the rotating frame. A 90° pulse on the coupling partner interchanges the α and β labels for just one-half of the spins, leaving two sets of antiphase vectors 'locked' into a configuration from which they cannot escape by free precession alone (Fig. 1). During this period no signal can be induced in the receiver coil but some *entity* ('double-quantum coherence') certainly evolves with time and can eventually be reconverted into observable magnetization by a radiofrequency pulse. This is where the product operator formalism comes into its own; we forsake geometrical pictures for an algebraic notation, a sure sign that we have a less intimate understanding of the problem.

REFERENCES

1. F. Bloch, *Phys. Rev.* **102**, 104 (1956).
2. A. Abragam, *The Principles of Nuclear Magnetism.* Oxford University Press, 1961.
3. M. H. Levitt and R. Freeman, *J. Magn. Reson.* **33**, 473 (1979).
4. G. A. Morris and R. Freeman, *J. Magn. Reson.* **29**, 433 (1978).
5 H. Geen and R. Freeman, *J. Magn. Reson.* **93**, 93 (1991).

Cross-references

Broadband decoupling
Composite pulses
Free induction decay
Multiple-quantum coherence
Nuclear Overhauser effect
Phase cycling
Product operator formalism
Pulsed field gradients
Radiofrequency pulses
Rotating frame
Selective excitation
Spin echoes
Spin–lattice relaxation
Spin–spin relaxation